McMule – a Monte Carlo generator for low energy processes

Yannick Ulrich[1]

[1]Institut für Theoretische Physik & AEC, Universität Bern, Sidlerstrasse 5, CH-3012 Bern, Switzerland

E-mail: yannick.ulrich@cern.ch

Abstract. McMule, a Monte Carlo for MUons and other LEptons, implements many major QED processes at NNLO (eg. $ee \to ee$, $e\mu \to e\mu$, $ee \to \mu\mu$, $\ell p \to \ell p$, $\mu \to \nu\bar{\nu}e$) including effects from the lepton masses, making it suitable for predictions for low-energy experiments such as MUonE, CMD-III, PRad, or MUSE.

Recently, McMule gained the ability to generate events at NNLO rather than just pre-defined differential distributions. To avoid negative event weights, it employs cellular resampling directly as part of the generation step which further reduces the fraction of negative weights.

1 Introduction

Higher-order QED corrections have become important for a number of measurements. Examples include luminosity measurements at e^+e^- colliders, tau physics, and measurements of the proton radius. Another central use case is the extraction of the hadronic vacuum polarisation contributions to the anomalous magnetic moment of the muon either in $e^+e^- \to$ hadrons or in $e\mu \to e\mu$. In the latter case, the MUonE experiment has an unprecedented precision goal of 10^{-5}. Finally, searches for New Physics in lepton decays, most notably $\mu \to e\gamma$ and $\mu \to eee$, require very good modelling of the Standard Model (SM) background.

In these proceedings, we will review McMule [1], a Monte Carlo for MUons and other LEptons. We have implemented all leptonic $2 \to 2$ processes in QED at next-to-next-to-leading order (NNLO) as well as a few others; a full list is shown in Table 1. Once provided with the required matrix elements, the McMule framework can calculate a physical cross section for an arbitrary physical, i.e. IR finite, observable. In doing so, it takes care of the phase space generation, subtraction [2], stabilisation [3], and integration.

The current stable version of McMule `v0.5.0` is an integrator which means it can calculate arbitrary distributions but not generate events. An event generator is currently still in testing as we will discuss below. The code can be obtained from

    https://mule-tools.gitlab.io

and the manual, which includes a getting started section, can be found at

    https://mcmule.readthedocs.io

The code is written in Fortran 95, compiled with `meson+ninja`, and supported by tooling in `python 3.9`. The user specifies their observable in a routine that is compiled separately and loaded at runtime, allowing them to use whatever language and framework they prefer.

process	experiment	physics motivation	order	reference
$e\mu \to e\mu$	MUonE	HVP to $(g-2)_\mu$	NNLO+	[1, 4]
$\ell p \to \ell p$	P2, Muse, Prad, QWeak, ...	proton radius, weak charge	NNLO	[1, 5]
$e^-e^- \to e^-e^-$	Prad 2	normalisation	NNLO	[6]
	MOLLER, ...	$\sin^2\theta_W$ at low Q^2		
$e^+e^- \to e^+e^-$	any e^+e^- collider	luminosity measurement	NNLO	[3]
$ee \to \ell\ell$	VEPP, BES, Daphne, ...	R-ratio	NNLO±	[7]
	Belle	τ properties		
$ee \to \gamma\gamma$	Daphne	dark searches	NNLO−	
	any e^+e^- collider	luminosity measurement		
$e\nu \to e\nu$	DUNE	flux & $\sin^2\theta_W$	NNLO−	
$\mu \to \nu\bar{\nu}e$	MEG	ALP searches	NNLO+	[8]
	DUNE	beam-line profiling		
$\mu \to \nu\bar{\nu}e\gamma$	MEG, Mu3e, Pioneer	background	NLO	[9]
$\mu \to \nu\bar{\nu}eee$	Mu3e	background	NLO	[10]
$ee \to \pi\pi$	VEPP, BES, Daphne, ...	R-ratio	NNLO−	
$ee \to \ell\ell\gamma$	VEPP, BES, Daphne, ...	R-ratio	NLO+	

Table 1: Processes included in MᴄMᴜʟᴇ, the experiment and physics case for which they are relevant, and the order at which they are implemented. A + indicates that future improvements are to be expected for this process, while a − indicates that this process is not known exactly at the given order.

These proceedings are organised as follows: in Section 2, we will very briefly review some of the theory behind MᴄMᴜʟᴇ to the extent that is relevant for its implementation. Next, we will discuss how MᴄMᴜʟᴇ's event generation mode will work in Section 3 with some results for $\mu \to \nu\bar{\nu}e$ at NNLO before concluding in Section 4.

2 Theory behind MᴄMᴜʟᴇ

To calculate a process in MᴄMᴜʟᴇ, it needs to know the relevant matrix elements (squared). Using $\mathcal{M}_n^{(\ell)}$ to denote the ℓ-loop n-particle matrix element, we need at

$$
\begin{array}{ll}
\text{LO} & \mathcal{M}_n^{(0)}, \\
\text{NLO} & \mathcal{M}_n^{(1)} \text{ and } \mathcal{M}_{n+1}^{(0)}, \\
\text{NNLO} & \mathcal{M}_n^{(2)}, \mathcal{M}_{n+1}^{(1)}, \text{ and } \mathcal{M}_{n+2}^{(0)}.
\end{array}
$$

These are represented as function pointers in MᴄMᴜʟᴇ and can come from any source. For the real-virtual $\mathcal{M}_{n+1}^{(1)}$, we usually rely on OpenLoops [11, 12] supplemented with an automatic stabilisation technique called next-to-soft (NTS) stabilisation [3] in numerically delicate situations. MᴄMᴜʟᴇ is further able to automatically construct the necessary counter terms and perform the numerical integration using the FKS$^\ell$ subtraction scheme.

2.1 The FKS$^\ell$ subtraction scheme

The calculation of higher-order corrections includes divergent real corrections. Since MᴄMᴜʟᴇ utilises numerical integration, we need to include a prescription to handle these in dimensional regularisation. Since we always consider fermions massive, the only source of singularities are soft emissions, where we can use the universal behaviour studied by Yennie, Frautschi, and Suura (YFS) [13]: a real-emission matrix element with any number of loops can be approximated in the limit of the emitted photon becoming soft as

$$
\mathcal{M}_{n+1}^{(\ell)} = \mathcal{E}\mathcal{M}_n^{(\ell)} + \mathcal{O}(\xi^{-1}), \tag{1}
$$

where we have defined the rescaled photon energy $\xi = 2E_\gamma/\sqrt{s}$. We have further defined the eikonal factor $\mathcal{E}$

$$
\mathcal{E} = -\sum_{ij} Q_i Q_j \frac{p_i \cdot p_j}{(p_i \cdot p_\gamma)(p_j \cdot p_\gamma)}, \tag{2}
$$

that considers all pairs of fermions with momenta p_i (assumed incoming) and charges Q_i. Integrating $\mathcal{E}$ over the phase space of the soft, unresolved photon results in the integrated eikonal $\hat{\mathcal{E}}$, which contains an explicit $1/\epsilon$ soft singularity. The YFS theorem further states that soft singularities exponentiate such that all singularities from loop integration can be subtracted by $\hat{\mathcal{E}}$ as follows

$$e^{\hat{\mathcal{E}}} \sum_{\ell=0}^{\infty} \mathcal{M}_n^{(\ell)} = \sum_{\ell=0}^{\infty} \mathcal{M}_n^{(\ell)f} = \text{finite}. \tag{3}$$

We can use (1) and (3) to construct an all-order extension of the FKS subtraction scheme [14, 15] called FKS$^\ell$ [2] that only requires knowledge of $\mathcal{E}$ and $\hat{\mathcal{E}}$ which allows for very efficient implementation. In particular, we have

$$\sigma^{(\ell)} = \sum_{j=0}^{\ell} \int d\Phi_{n+j} \frac{1}{j!} \left[\prod_{i=1}^{j} \left(\frac{1}{\xi_i} \right)_c \right] \mathcal{M}_{n+j}^{(\ell)f} \tag{4}$$

$$\int_0^1 d\xi \left(\frac{1}{\xi_i} \right)_c \equiv \int_0^1 d\xi \frac{f(\xi) - f(0)\theta(\xi_c - \xi)}{\xi}, \tag{5}$$

where we have also defined an unphysical parameter $0 < \xi_c \leq 1$ that can be chosen arbitrarily.

2.2 NTS stabilisation

To improve the numerical stability and performance when a real photon becomes soft, we utilise NTS stabilisation. The basic idea is to expand the matrix element $\mathcal{M}_{n+1}^{(1)}$ in the photon energy ξ up to next-to-leading power (NLP) and use the expanded result rather than the full OpenLoops calculation. While the leading power (LP) term is just the eikonal of (1), the next term is more complicated. It was first studied by Low [16], Burnett, and Kroll [17] at tree level as the LBK theorem and later extended first to one-loop [18] and later to any number of loops [19] and photons [20]. The case relevant for the real virtual is

$$\mathcal{M}_{n+1}^{(1)} = \underbrace{\mathcal{E} \times \mathcal{M}_n^{(1)}}_{\text{LP}} + \underbrace{D_{\text{LBK}}\left[\mathcal{M}_n^{(1)} \right] + \mathcal{S} \times \mathcal{M}_n^{(0)}}_{\text{NLP}} + \mathcal{O}(\xi^0). \tag{6}$$

For the exact definitions of the LBK operator D_{LBK} and the soft function $\mathcal{S}$, see for example [19]. The former is a differential operator that is acting on the one-loop matrix element $\mathcal{M}_n^{(1)}$. This operator can be very neatly written in terms of shifted kinematics [21, 22] that can be chosen to fulfil on-shellness and momentum conservation exactly [23]. This is also true for polarised scattering, albeit with some subtleties [7]. The soft function $\mathcal{S}$ is similar to the eikonal $\mathcal{E}$ except that it has a sum over three partons rather than two.

Since all matrix elements are presumed to be known in MCMULE it is hence possible to implement (6) by only knowing the momenta and charges of the particles involved without any process-dependent calculations.

3 Event generation

The techniques and tools described so far are sufficient to calculate any fixed-order differential distribution. However, to model experiments with a Monte Carlo, we need to be able to generate events as well. The naive 'garden hose' approach of just storing the sampled momenta and weights is suboptimal. Since we are using a subtraction scheme, many events will end up with negative weight. These are not in and of themselves a problem but increase the number of samples required to reach a given statistical error. A naive estimate would suggest that if $r \times N$ of N weights are negative, we would need $\propto 1/(1-2r)^2$ more events to reach the same precision. If the events are just quickly histogrammed this is not too big of an issue. However, if, for example, they are propagated through a costly experimental detector simulation, the number of events needs to be minimised. In practice, this means we need to cancel the negative events early as part of the Monte Carlo rather than late in the histogram.

To do this, MCMULE implements a technique called cellular resampling [24, 25]. This method is based on two central ideas

- integrated cross section are positive, *regardless of the size of the integration domain* $\mathcal{C}$

$$\sigma_{\mathcal{C}} = \int_{\mathcal{C}} \mathrm{d}\sigma > 0 \,, \tag{7}$$

- experiments have finite resolution.

By combining these two facts, we arrive at the resampling algorithm of [24, 25]

1. Generate events.

2. Pick the event with the most negative weight $w_i < 0$ as a seed for a cell $\mathcal{C}$.

3. Find nearby events and add them to $\mathcal{C}$. This nearest neighbour search can be performed efficiently using vantage-point trees [26, 27].

4. Repeat until either:

   - the cell becomes too large and events in it become resolvable. In this case, keep w_i negative
   - the total weight is positive

$$\sum_{i \in \mathcal{C}} w_i > 0 \,. \tag{8}$$

   In this case, reweight

$$w_i \to \frac{\sum_{j \in \mathcal{C}} w_j}{\sum_{j \in \mathcal{C}} |w_j|} w_i \tag{9}$$

5. Go back to Step 2 until no more events can be resampled.

An animation of this procedure can be found in the supplementary materials to this submission.

If the original number of events was high enough, this algorithm is guaranteed to remove all negative weights without biasing any physical observable. However, this is often difficult to achieve in practice. Hence, we extend this algorithm by one more step

6. Generate more events in all cells that still contain a negative weight.

This is possible because we are using cellular resampling as part of the generator rather than as a post-processor for an already existing set of events.

To make use of the cellular resampling algorithm, we need to define a distance in event space. This metric must ensure that events that differ only by soft photons are considered close to each other (IR safety) and ideally also considers events that are similar to be close to each other.

In the case of $\mu \to \nu\bar{\nu}e$ where only the electron is detected, a suitable metric might be

$$d(e_1, e_2) = \sqrt{\left| 2E_e^{(1)}/m_\mu - 2E_e^{(2)}/m_\mu \right|^2 + \left| \cos\theta_e^{(1)} - \cos\theta_e^{(2)} \right|^2} \,, \tag{10}$$

though further kinematic information may be added as required. In Figure 1 we show the size of the corrections for the energy spectrum of the electron at NLO and NNLO both with and without resampling. The resampling reduces the fraction of negative weights from

$$r \approx 2 \times 10^{-2} \to 2 \times 10^{-5} \,. \tag{11}$$

Further, the "badness" of the negative weights also gets reduced. To quantify this we compare the worst weight $w_{\min}$ with the average weight $\langle w \rangle$

$$\frac{w_{\min}}{\langle w \rangle} \approx -10^5 \to -10^{-3} \,. \tag{12}$$

This indicates that cellular resampling successfully handles the problem of negative events, allowing McMule to generate events that are well-suited for experimental studies.
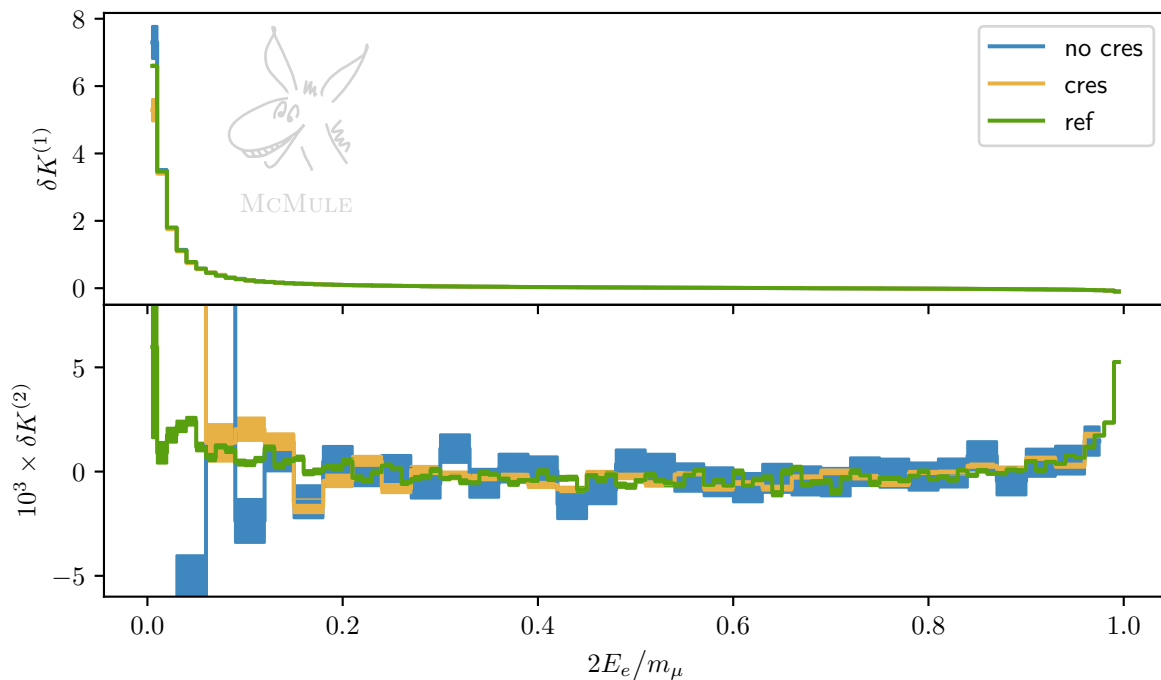
Figure 1: The results for the differential K factor $\delta K^{(i)} = (\mathrm{d}\sigma^{(i)}/\mathrm{d}x)\big/(\mathrm{d}\sigma^{(i-1)}/\mathrm{d}x)$ for the energy fraction of the electron $x = 2E_e/m_\mu$ in $\mu \to e\nu\bar{\nu}$. McMule ran in the default mode ("ref"), event generator mode ("no cres") and cell-resampling mode ("cres").

4 Conclusion

In these proceedings we have discussed the McMule framework for higher-order QED calculations. We further introduced the event generation aspect and demonstrated cellular resampling as part of a Monte Carlo tool. While already well established for NNLO-QED, we plan to extend our code to include more processes such as $e\mu \to e\mu\gamma$ at NNLO, $eN \to eN$ for various nuclei such as carbon or deuterium as well as $ee \to \pi\pi$. We are also working on the inclusion of electroweak effects for $ee \to ee, \mu\mu$ at NNLO.

References

[1] P. Banerjee, T. Engel, A. Signer and Y. Ulrich, *QED at NNLO with McMule, SciPost Phys.* **9** (2020) 027 [2007.01654].

[2] T. Engel, A. Signer and Y. Ulrich, *A subtraction scheme for massive QED, JHEP* **01** (2020) 085 [1909.10244].

[3] P. Banerjee, T. Engel, N. Schalch, A. Signer and Y. Ulrich, *Bhabha scattering at NNLO with next-to-soft stabilisation, Phys. Lett. B* **820** (2021) 136547 [2106.07469].

[4] A. Broggio et al., *Muon-electron scattering at NNLO, JHEP* **01** (2023) 112 [2212.06481].

[5] T. Engel, F. Hagelstein, M. Rocco, V. Sharkovska, A. Signer and Y. Ulrich, *Impact of NNLO QED corrections on lepton-proton scattering at MUSE, Eur. Phys. J. A* **59** (2023) 253 [2307.16831].

[6] P. Banerjee, T. Engel, N. Schalch, A. Signer and Y. Ulrich, *Møller scattering at NNLO, Phys. Rev. D* **105** (2022) L031904 [2107.12311].

[7] S. Kollatzsch and Y. Ulrich, *Lepton pair production at NNLO in QED with EW effects*, *SciPost Phys.* **15** (2023) 104 [2210.17172].

[8] P. Banerjee, A. Coutinho, T. Engel, A. Gurgone, A. Signer and Y. Ulrich, *High-precision muon decay predictions for ALP searches*, *SciPost Phys.* **15** (2023) 021 [2211.01040].

[9] G.M. Pruna, A. Signer and Y. Ulrich, *Fully differential NLO predictions for the radiative decay of muons and taus*, *Phys. Lett. B* **772** (2017) 452 [1705.03782].

[10] G.M. Pruna, A. Signer and Y. Ulrich, *Fully differential NLO predictions for the rare muon decay*, *Phys. Lett. B* **765** (2017) 280 [1611.03617].

[11] F. Buccioni, S. Pozzorini and M. Zoller, *On-the-fly reduction of open loops*, *Eur. Phys. J. C* **78** (2018) 70 [1710.11452].

[12] F. Buccioni, J.-N. Lang, J.M. Lindert, P. Maierhöfer, S. Pozzorini, H. Zhang et al., *OpenLoops 2*, *Eur. Phys. J. C* **79** (2019) 866 [1907.13071].

[13] D.R. Yennie, S.C. Frautschi and H. Suura, *The infrared divergence phenomena and high-energy processes*, *Annals Phys.* **13** (1961) 379.

[14] S. Frixione, Z. Kunszt and A. Signer, *Three jet cross-sections to next-to-leading order*, *Nucl. Phys. B* **467** (1996) 399 [hep-ph/9512328].

[15] R. Frederix, S. Frixione, F. Maltoni and T. Stelzer, *Automation of next-to-leading order computations in QCD: The FKS subtraction*, *JHEP* **10** (2009) 003 [0908.4272].

[16] F.E. Low, *Bremsstrahlung of very low-energy quanta in elementary particle collisions*, *Phys. Rev.* **110** (1958) 974.

[17] T.H. Burnett and N.M. Kroll, *Extension of the low soft photon theorem*, *Phys. Rev. Lett.* **20** (1968) 86.

[18] T. Engel, A. Signer and Y. Ulrich, *Universal structure of radiative QED amplitudes at one loop*, *JHEP* **04** (2022) 097 [2112.07570].

[19] T. Engel, *The LBK theorem to all orders*, *JHEP* **07** (2023) 177 [2304.11689].

[20] T. Engel, *Multiple soft-photon emission at next-to-leading power to all orders*, *JHEP* **03** (2024) 004 [2311.17612].

[21] D. Bonocore and A. Kulesza, *Next-to-leading power corrections for soft photon bremsstrahlung*, *PoS* **ICHEP2022** (2022) 1128.

[22] R. Balsach, D. Bonocore and A. Kulesza, *Soft-photon spectra and the LBK theorem*, 2312.11386.

[23] R. Balsach, A. Kulesza and D. Bonocore, *The Emission of Soft-photons and the LBK Theorem, Revisited*, *Acta Phys. Polon. Supp.* **17** (2024) 2 [2401.01820].

[24] J.R. Andersen and A. Maier, *Unbiased elimination of negative weights in Monte Carlo samples*, *Eur. Phys. J. C* **82** (2022) 433 [2109.07851].

[25] J.R. Andersen, A. Maier and D. Maître, *Efficient negative-weight elimination in large high-multiplicity Monte Carlo event samples*, *Eur. Phys. J. C* **83** (2023) 835 [2303.15246].

[26] J.K. Uhlmann, *Satisfying general proximity/similarity queries with metric trees*, *Inf. Process. Lett.* **40** (1991) 175.

[27] P.N. Yianilos, *Data structures and algorithms for nearest neighbor search in general metric spaces*, in *Proceedings of the Fourth Annual ACM-SIAM Symposium on Discrete Algorithms*, SODA '93, (USA), p. 311–321, Society for Industrial and Applied Mathematics, 1993.